2024 IEEE/RSJ International Conference on Intelligent Robots and Systems (IROS)
October 14-18, 2024. Abu Dhabi, UAE

An Origami-Inspired Pneumatic Continuum Module with Active Variable Stiffness

Zhuowen Li, Huaiyuan Chen*, Fan Xu*, Hesheng Wang

***Abstract*— This paper presents a novel pneumatic continuum module featuring high contraction-ratio, bidirectional actuation, and active stiffness regulation. The module comprises four linear pneumatic actuators integrating rigid polygon origami frame into soft bellow. This integration not only helps to regulate motion but also enhances structural strength, facilitating contraction and bending performance. The contraction resulting from vacuum pressure serves as a limiting layer for one opposing pair of actuators, while the other pair operates in a virtual antagonistic configuration, allowing for active regulation of joint stiffness through pressure control. The paper provides a detailed workflow covering the design, fabrication, and mathematical modeling of the pneumatic module. Furthermore, the paper presents verifications of the module's actuation capacity and active variable stiffness. The findings of this study can serve as valuable references for the design of manipulators.**

I. Introduction

Pneumatic continuum manipulators can produce motion through continuous deformation of the soft mechanism, the motion mode of which gains inspiration from biological parts [1]–[3]. The advantages of increasing flexibility, environmental adaptability and compliant interactions bring the continuum manipulators closer to human-robot collaborations. Despite the well-known advantages of soft continuum robots in safe interactions, finding the right balance between compliance for interaction and maintaining competency in substantial-load tasks remains a challenge yet to be addressed in mechanism design and fabrication [4]. Hence, besides the primary considerations of actuation range and output force in designing pneumatic continuum manipulators, the need for active stiffness regulation arises as an additional requirement to strike a balance between compliance and load capacity.

The working principles for variable stiffness can be mainly divided into two classes, namely, jamming method and antagonistic method [4]. The jamming method is to modify the comprised elements interactions. Applying pressure or vacuum forces the particles into tighter or looser contacts, allowing for the adjustment of stiffness accordingly [5]. The researches have adopted jamming method because of the advantages of easy implementation and reversibility [6]–[9]. However, the filled materials for particles will add extra weight to the system and prolong the recovery time, resulting in a bulky mechanism and introducing new challenges in practical applications.

The antagonistic method is another widely adopted solution for achieving variable stiffness. Inspired by the musculoskeletal system, antagonistically arranged muscles can adjust the stiffness of limbs to achieve precise force control when handling objects [10]. This kind of antagonistic actuation is achieved by two or more sets of muscles/actuators collaborating in an opposing way to actuate a joint or a structure. Researchers have used a combination of different active actuation technologies to propose a variable stiffness manipulator. The use of rigid structures is an effective way to enable variable stiffness with antagonistic method. The hybrid design by fixing pneumatic actuators into hinge joints can improve the control accuracy and structure strength [11]–[14]. The stiffness and position control of each joint is obtained through adjusting the pressures for one pair of pneumatic actuators. The pressure difference contributes to position control, while the average pressure influences the stiffness. The rigid joint brings convenience to decouple the stiffness control from position. However, these continuum manipulators reserve the characteristics of rigid manipulators driven by electric motors. The lack of flexibility and adaptability of such designs impedes further applications in certain complex environments.

A soft pneumatic continuum manipulator without rigid structures may be less capable of satisfactorily adjusting stiffness actively with antagonistic method. In this light, the limiting layer or tendons are the solution to realize variable stiffness. The air chambers are set with circle-array configuration to constitute the antagonistic actuation. The limiting layer or tendons works as the virtual joint. When inflating the bending/extending actuator and tensioning the layer or tendons at the same time, an antagonistic effect is producing, thus variable stiffness can be achieved [15]–[19]. But these limiting tendons are mainly driven by electric motors. Another alternative to form the tendon is using a pneumatic extending/contracting actuator, which simplifies the hardware system for unified types of actuation [4], [20], [21]. The pneumatic actuator for limiting tendon often generates opposite actuation to achieve active force balance. Because the flexible structure, these manipulators are suitable for complex application. However, the limited contraction ratio restricts the workspace of manipulator. And the load capacity is another issue to be addressed for these designs.

To sum up, this paper proposes an origami-inspired pneumatic continuum module featuring at contraction-ratio, bidirectional actuation and variable stiffness. The continuum

This work was supported by the Natural Science Foundation of China (Grant 62203298). (Corresponding author: Fan Xu and Huaiyuan Chen)

Z. W. Li is with School of Mechanical Engineering, H. Y. Chen, F. Xu and H. S. Wang are with School of Electronic Information and Electrical Engineering, the Department of Automation, Shanghai Jiao Tong university(e-mail: lizhuowen@sjtu.edu.cn, chynh123@sjtu.edu.cn, xufanlyra@sjtu.edu.cn, wanghesheng@sjtu.edu.cn)

module consists of four linear pneumatic actuators with rigid origami film integrated into each soft bellow. The origami frame can mitigate the nonlinearity ubiquitous in the soft mechanism, thereby enabling easier motion regulation. Moreover, it can also improve the structural strength, facilitating the active stiffness changing ability through antagonistic deployment. The contributions are as follows:

1) The design of the continuum module and the origami-inspired pneumatic actuator, along with fabrication details, are presented in this paper;

2) The mathematical model is proposed to theoretically analyze the actuation characteristics and the associated load capacity, followed by cross-validations;

3) The principle of active stiffness regulation for the continuum module is presented and the stiffness changing ability has been verified across various cases.

The rest of this paper is organized as follows: Section II presents the design and fabrication of continuum module; In section III, the modeling of output force and the variable stiffness principle are introduced; Section IV presents the verification and Section V presents the conclusion.

II. Design and Fabrication

A. Design of the continuum module

The continuum module comprises four linear pneumatic actuators arranged in a circular array, as illustrated in Fig. 1. The pressure of each actuator is regulated, contributing to controlling 3-DOF spatial motion of the continuum module, including extension/contraction and 2-DOF bendings.

To construct a single pneumatic actuator, the origami-inspired design based on previous work, is employed [22]. The thin origami frame is designed using a polygon pattern of n_1 sides to achieve isotropic behavior of actuator. The polygon pattern has two main structural parameters: the circumradius of the polygon r and the length of the side edge b. The single actuator is constructed by aligning n_2 origami-based segments in linear array. With the integrated polygon origami frame, the structural strength is improved to withstand negative pressure, enabling contracting actuation capacity. Consequently, the bidirectional actuation, which includes extension under pressurization and contraction under vacuum is enabled. With restricted air flow, a single actuator is able to maintain its length. The virtual joint axis can be constructed by restricting one pair of opposite actuators, and the remaining pair of actuators constitutes antagonistic configuration, enabling active stiffness changing.

B. Fabrication procedures

The actuator is constructed by integrating the frame of the polygon pattern into the soft bellow. To guarantee both structural strength and contraction-ratio simultaneously, the ideal material for the frame should be thin, high-strength and capable of withstanding numerous folds. To this end, the 0.4mm polyvinyl chloride (PVC) film is selected. For the external bellow, fabric with high tensile strength is the applicable material, and the thermoplastic polyurethanes (TPU) fabric is utilized. The layered fabrication is then

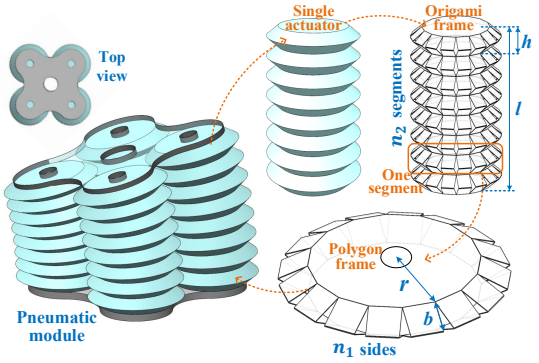

Fig. 1. Design of the pneumatic continuum module and the single origami-inspired actuator.

employed for the single pneumatic actuator, as depicted in Fig. 2.

The laser cutting is firstly used to construct the origami film. Dashed lines from pulse laser cutting for the creases would reduce the bending stiffness and induce the PVC film to fold in these lines. The 20mm/s cutting speed, 14% of the rated power, 1.5mm pulse cutting interval and 0.7mm cutting length are selected using laser cutting machine(BF1390+, Kaitian). And two holes are cut out to enable the air flow between adjacent segments.

The double-side tape is used to adhere the processed PVC film to the 0.06mm TPU fabric with larger circular area. The TPU fabric contains two layers, i.e., the TPU layer and the high-strength Nylon layer. The TPU layer is set as inner side of air chamber which contacts PVC film. The fabric along PVC periphery is heat-sealed to construct single chamber, as is illustrated with highlighted circular ring in Fig. 2(b).

All the air chambers are connected by adhering circular areas in Fig. 2(c) with instant glue(5562, Youweite). The vents should be aligned to guarantee fluent air flow. Then the continuum module is constituted with four actuators.

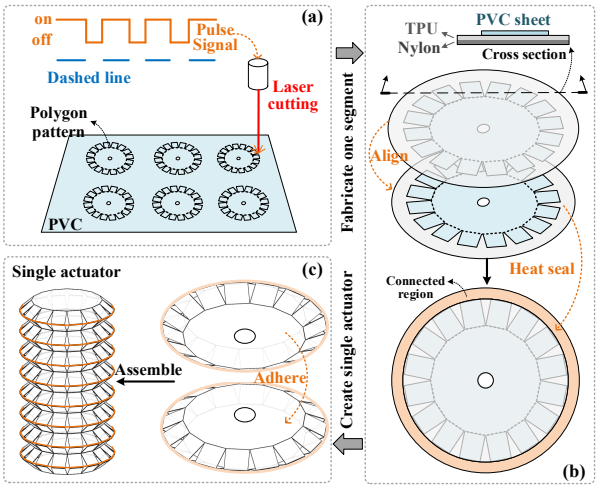

Fig. 2. Layered fabrication of single actuator, (a)Laser-cutting the Polygon origami frame out of PVC film, (b)Heat-healing the composite sheet into one segment, (c)Assembling several segments through adhesion into single pneumatic actuator.

III. Modeling and Working Principle

A. Modeling for single actuator

The load capacity of a single actuator (also known as the output force exerted by the actuator to the external) is modeled related to the system geometry and the actuation. The internal volume is firstly derived. On account of the origami frame for each segment, the volume can be calculated with simple geometry. Each segment is comprised of one hexadecimal prism, sixteen triangular prisms, and sixteen tetrahedrons. Clearly, when the height of segment is given, the geometric shape of the segment is totally defined by the parameters of origami pattern. Thus, the volume for hexadecimal prism, triangular prism and tetrahedron are:

$$v_1 = \frac{n_1 r^2 h \cdot \sin\alpha}{2} \tag{1}$$

$$v_2 = n_1 \sqrt{b^2 - \frac{h^2}{4}} hr \cdot \sin\frac{\alpha}{2} \tag{2}$$

$$v_3 = \frac{n_1(4b^2 - h^2)h \cdot \sin\alpha}{24} \tag{3}$$

where $\alpha = 2\pi/n_1$ denotes the central angle of the hexadecagon and h denotes the height of the segment. Then the volume of one segment can be derived by adding v_1,v_2 and v_3 up. Because each actuator has n_2 segments, the total volume V of single actuator can be obtained as follow:

$$\begin{aligned} V &= n_2\left(v_1 + v_2 + v_3\right) \\ &= \frac{n_1 r^2 \sin\alpha}{2} \cdot l + n_1 \sqrt{b^2 - \frac{l^2}{4n_2^2}} \cdot r \sin\frac{\alpha}{2} \cdot l \\ &\quad + \frac{n_1\left(4n_2^2 b^2 - l^2\right)\sin\alpha}{24n_2^2} \cdot l \end{aligned} \tag{4}$$

where $l = n_2 \cdot h$ denotes the length of actuator. In order to establish the quasi-static model, the virtual work theory [23] is used to reveal the relationship between the pressure and the length of actuator:

$$(F_{ex} + F_{spr}(l)) \cdot dl = pdV \tag{5}$$

where F_{ex} is the external force, $F_{spr}(l)$ is the force function of hypothetical equivalent spring. p is the gauge pressure of actuator and V represents the volume of a actuator. Then, substituting the volume model and the virtual work theory, the expression of pneumatic force is obtained as follows:

$$\begin{aligned} F_p &= F_{ex} + F_{spr}(l) \\ &= p \cdot (-\frac{n_1 l^2 \sin\alpha}{8n_2^2} + n_1 r \sin\left(\frac{\alpha}{2}\right) \frac{2n_2^2 b^2 - l^2}{n_2\sqrt{4n_2^2 b^2 - l^2}} \\ &\quad + \frac{n_1\left(3r^2 + b^2\right)\sin\alpha}{6}) \end{aligned} \tag{6}$$

where F_p represents the thrust or contraction force generated by gauge pressure in the actuator, which balances with external force and spring's force. From Eq.(6) the output force can be predicted according to pressure and geometry parameters of actuator.

B. Principle for variable stiffness

The pose of the continuum module is controlled by regulating the length of each actuator through internal pressure. By introducing antagonistic motion between two pairs of actuator, the bending and contraction stiffness can also be actively regulated, as illustrated in Fig. 3.

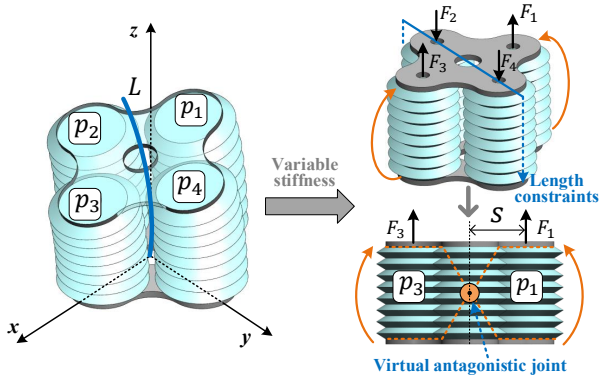

Fig. 3. Working principle for variable bending stiffness.

For bending stiffness, the antagonistic motion is generated by a virtual joint comprising a pair of opposite actuators (i.e., actuator 2 and actuator 4 in Fig. 3), which constrains the motion of the remaining pair by limiting the airflow or blocking the length. With constrained length for actuator 2 and actuator 4, the continuum module turns into a joint driven by actuator 1 and actuator 3 in antagonistic configuration [24]. The virtual joint is radial central axis throughout actuator 2 and actuator 4. Apart from bending stiffness, the contraction stiffness can also be achieved through antagonistic method. For specific module length, different combinations of pressurization for actuator 1, 3 and vacuum for actuator 2, 4 can achieve different force balance. These different force balance states with same module length can result in different contraction/extension stiffness. Consequently, the bending stiffness k_θ and contraction stiffness k_l can be actively regulated through actuators' pressure:

$$\begin{aligned} k_\theta &= \frac{\partial T}{\partial\theta} = \frac{\partial(s \cdot (F_1 - F_3))}{\partial\theta} \\ &= s \cdot (\frac{\partial F_1}{\partial l_1}\frac{\partial l_1}{\partial\theta} - \frac{\partial F_3}{\partial l_3}\frac{\partial l_3}{\partial\theta}) \end{aligned} \tag{7}$$

$$k_l = \frac{\partial F}{\partial l} = \frac{\partial(F_1 + F_3 + F_2 + F_4)}{\partial l} \tag{8}$$

where $F_i = p_i \cdot (dV_i/dl_i) - F_{spr}(l_i)$ represents the force generated from the actuator i $(i = 1, 2, 3, 4)$. When the force is a contraction force, F_i is negative. When the force is a thrust force, F_i is positive. T represents the deflection torque by F_i with moment arm s. And θ represents the deflection angle. Considering that $\partial l_1/\partial\theta = s$ and $\partial l_3/\partial\theta = -s$, the expression is turned into:

$$\begin{cases} k_\theta = s^2 \cdot (p_1 \dfrac{d^2V_1}{dl_1^2} + p_3 \dfrac{d^2V_3}{dl_3^2} - k_1 - k_3) \\ k_l = \sum_{i=1}^{4} p_i \cdot \dfrac{d^2V_i}{dl^2} - \sum_{i=1}^{4} k_i \end{cases} \tag{9}$$

where $k_i = dF_{spr}(l_i)/dl_i$ represents the structure stiffness of actuator i at specific length. Therefore, the stiffness can then be controlled by regulating the pressure of actuators. Similarly, when the lengths of actuators 1 and 3 are constrained, actuators 2 and 4 operate antagonistically to control the stiffness of the module.

IV. Verification

For the origami-inspired pneumatic actuator and continuum module, a set of empirical parameters is selected, as shown in Table I. Using the layered fabrication, the actuator with given parameters and the continuum module with 8 segments are shown in Fig. 4. The linear actuation range is 17.0-119.4mm, indicating the contraction ratio of 85.7%. Several experiments have been conducted to evaluate the actuation characteristics and stiffness changing performance.

TABLE I
THE PARAMETERS FOR ORIGAMI PATTERN.

Symbol	Quantity	Value
n_1	number of sides in the polygon	16
n_2	number of segments	8
r	circumradius of the polygon	16.9mm
b	length of side edge	8mm

Fig. 4. Fabricated continuum module from origami-inspired actuator.

A. Experimental setup

The experimental evaluation focuses on both the actuation characteristics including output force and bending behavior, and its stiffness regulation capability of the continuum module. The platform and the experimental setup are shown in Fig. 5(a), where the output force at different length and pressure is firstly measured. A linear block is used to set the pneumatic continuum module at specific length. The force sensor (SBT650, SIMBATOUCH) is used to measure the contraction/extension force. In addition, the pressure for each actuator is controlled using two switching valves (VQ100, SMC) driven by PWM signals: one for inflation and another for deflation, as is shown in Fig. 5(b). The proportional controller is applied to adjust the duty cycle of PWM for pressure control. The sensor (XGZ6847, CFSensor) is used for pressure measurement for each actuator. Two air compressors with 300kPa and -40kPa are used to drive the actuators under positive or negative pressures. All the pneumatic components are integrated in the control box shown in Fig. 5(c). Apart from linear characteristics, the bending behaviours and stiffness tuning performance are evaluated under motion capture system (Vero, Vicon).

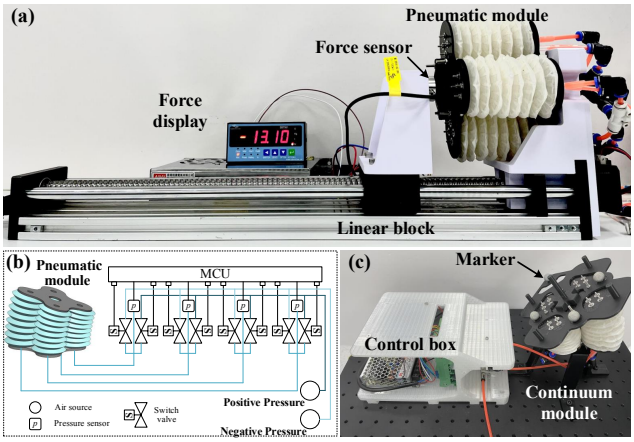

Fig. 5. Experimental platforms, (a)The tests for output force in linear block, (b)The pneumatic system to drive four actuators, (c)The tests for bending behavior and variable stiffness in motion capture system.

B. Actuation characteristics

This section concentrates on the validation of the proposed actuator model and test bending characteristics.

Firstly, the spring stiffness-related force $F_{spr}(l)$ is obtained as prior knowledge. Data on the equivalent spring stiffness are collected with varying actuator lengths at 0 kPa pressure. Leveraging function approximation techniques, $F_{spr}(l) = 4.1 \times 10^3 \cdot l^2 + 171.1 \cdot l$ is obtained ($R^2 = 0.998$), as illustrated in Fig. 6(a). The spring stiffness increases with actuator length and the quadratic polynomial can describe the stiffness force.

The force from actuation pressure at different length can be found in Fig. 6(b). Thrust force happens under pressurization and contraction force happens under vacuum. The thrust force is up to 126.4N at 0.02m/30kPa and the contraction force is up to 100.4N at 0.08m/-15kPa. It should be noted that, larger force can be achieved with larger pressure and the maximum pressure of 100kPa is detected. The force value increases with pressure value linearly, but decreases with actuator length, which can be explained from the mathematical modeling that dV/dl decreases with length. For better illustration, the linear force with varying pressure at given length is shown in Fig.6(c). Although with small deviations, the experimental force almost corresponds to the theoretical force from quasi-static model. Apart from force measurement, the tests of lifting different weights are also conducted, which can be found in supplemental video.

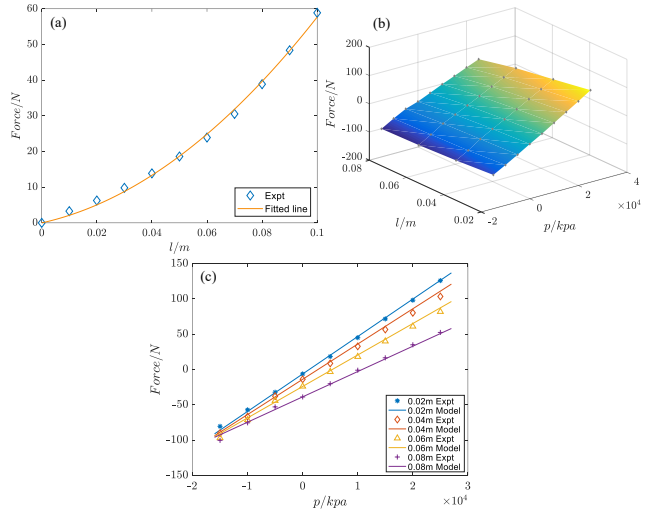

Fig. 6. Actuation characteristics, (a)The structure stiffness of the module (b)The force under different lengths and pressures, (c)The force under specific length and varying pressure.

The bending characteristics for proposed continuum module are tested with different pressure combinations. Two cross configurations, i.e., bending from single actuator and two adjacent actuators, have been tested respectively. Fig. 7(a) and 7(c) show the first one. The opposite actuator's pressure is set at 0kpa, 5kpa, 10kpa, 20kpa in different tests. The bending motion driven by adjacent actuators is similar to that driven by a single actuator. For larger force generated by two actuators, this configuration has the max bending angles about 75° under the condition of 0kPa and 30kPa combined. And it should be noted that larger workspace can be achieved through different combinations of pressure.

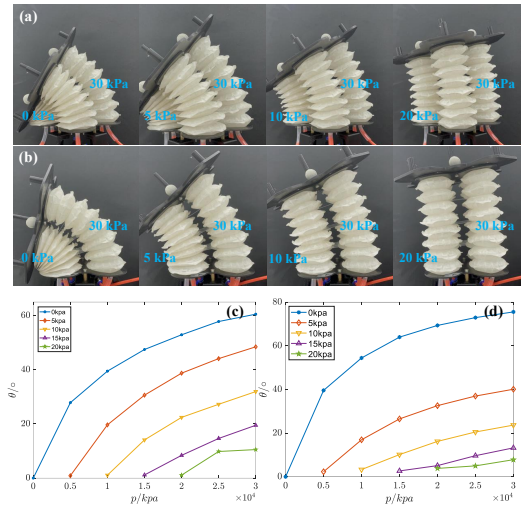

Fig. 7. The bending characteristics, (a), (c)Bending behaviour driven by single actuator; (b), (d)Bending behaviour driven by two adjacent actuators.

C. Variable stiffness

For bending stiffness, when the actuator 2 and 4 are constrained for the length, the stiffness is tuned through the pressure of actuator 1 and actuator 3 which are configured antagonistically. So we set the pressure of actuator 1 and 3 as following:

$$\begin{cases} p_1 = p_0 + \Delta p_1 \\ p_3 = p_0 + \Delta p_3 \end{cases} \tag{10}$$

The pressure difference Δp is used to control the bending angle of antagonistic joint, while the pressure p_0 determines the joint stiffness [25]. When Δp=0, θ=0 without external load. Increasing p_0 won't change bending angle, but will increase the joint stiffness k_θ. Then, different weights varying from 300g to 500g are fixed at the top of module with a given offset to generate deflection torque, resulting in a deflection angle θ. One pair of opposite actuators, i.e., actuator 2 and actuator 4 in Fig. 3, are constrained from air flow with all valves closed. For the other pair of actuators, the pressures are both controlled as p_0 varying from 5kPa to 30kPa to test the stiffness of the module. The deflection angle at varying conditions is shown in Fig. 8 and supplemental video. At specific weight, i.e., deflection torque, higher pressure p_0 make smaller deflection angle. Considering that (7), smaller deflection angle means higher stiffness k_θ. This suggests that the bending stiffness can be tuned by controlling the pressure.

It should be noted that because of interference between top and bottom plates the angle at 500g/5kPa is approximately equivalent to the angle at 500g/10kpa. For the constrained actuators, the length is stretched due to the thrust force exerted by antagonistic actuators. This is because we haven't measure the length of individual actuator, rendering us unable to control them. In order to address this coupling phenomenon, we will establish a means to measure and control individual actuator length in the future.

To measure the contraction stiffness, different weights varying from 300g to 500g are fixed at the center of the top of module to test the length change for stiffness, as is shown in Fig. 8(c). In addition, the module is maintained at a moderate length for stiffness testing under specific conditions. Actuators 2 and 4 are subjected to controlled pressures of 7kPa, 3kPa, -2kPa, -7kPa, and -11kPa for constraints, while actuators 1 and 3 undergo corresponding pressures of 8kPa, 13kPa, 18kPa, 23kPa, and 28kPa in sequence. Different combinations of pressure sets for actuators 1, 3 and actuators 2, 4 will make different force balance state. Likewise, the reduction in length change corresponds to an increase in pressure, indicating a positive correlation between stiffness and pressure p_0.

The ability to withstand vacuum enables the actuator to achieve bidirectional actuation, providing the basis for variable stiffness. This allows different equilibrium states to be attained through simultaneous extension and contraction.

V. Discussion and Conclusion

This paper proposes an origami-inspired pneumatic continuum module featuring high contraction ratio, bidirectional actuation and variable stiffness. The continuum module consists of four pneumatic actuators, integrating polygon origami

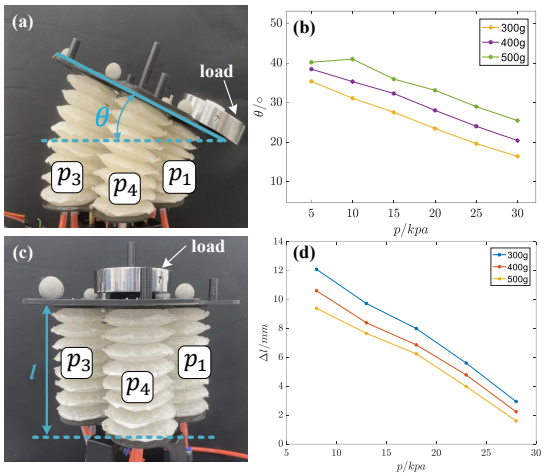

Fig. 8. The variable stiffness tests, (a)The setup for bending stiffness tests, (b)The deflection angle under different condition, (c)The setup for contraction stiffness tests, (d)The length change at different pressure of actuator 1 and 3.

film into soft bellow by layered fabrication. The origami film regulates motion and enhances structural strength to bear negative pressure, enabling bidirectional actuation of the continuum module. On the basis of mathematical model for single actuator, the principle of variable stiffness is introduced. With length-constrained actuators constructing the virtual axis, the other pair of actuators functions in antagonistic configuration to adjust the bending and contraction stiffness.

The verification including actuation characteristics and variable stiffness has been conducted. The module can deliver thrust force(up to 126N) and contraction force(up to 100N). In the tests assessing bending and contraction stiffness, it was observed that with increasing pressure, both the deflection angle and length change decrease, indicating a corresponding increase in bending and contraction stiffness. While other soft robots are capable of tuning stiffness, they often exhibit a low contraction ratio [20], [21]. In contrast, with contraction ratio of about 85.7%, our continuum module with compact design excels in both aspects.

In the future, the manipulator with multi modules embedding sensing devices will be designed. In addition, the kinematic and dynamic model will also be researched.

REFERENCES

[1] M. Russo, S. M. H. Sadati, X. Dong, A. Mohammad, I. D. Walker, C. Bergeles, K. Xu, and D. A. Axinte, "Continuum robots: An overview," *Advanced Intelligent Systems*, vol. 5, no. 5, p. 2200367, 2023.

[2] X. Chen, X. Zhang, Y. Huang, L. Cao, and J. Liu, "A review of soft manipulator research, applications, and opportunities," *Journal of Field Robotics*, vol. 39, no. 3, pp. 281–311, 2022.

[3] O. Sokolov, A. Hošovský, and M. Trojanová, "Design, modelling, and control of continuum arms with pneumatic artificial muscles: A review," *Machines*, vol. 11, no. 10, 2023.

[4] W. Dou, G. Zhong, J. Cao, Z. Shi, B. Peng, and L. Jiang, "Soft robotic manipulators: Designs, actuation, stiffness tuning, and sensing," *Advanced Materials Technologies*, vol. 6, no. 9, p. 2100018, 2021.

[5] L. Blanc, A. Delchambre, and P. Lambert, "Flexible medical devices: Review of controllable stiffness solutions," *Actuators*, vol. 6, no. 3, 2017.

[6] T. Ranzani, M. Cianchetti, G. Gerboni, I. D. Falco, and A. Menciassi, "A soft modular manipulator for minimally invasive surgery: Design and characterization of a single module," *IEEE Transactions on Robotics*, vol. 32, no. 1, pp. 187–200, 2016.

[7] Y. Li, Y. Chen, Y. Yang, and Y. Wei, "Passive particle jamming and its stiffening of soft robotic grippers," *IEEE Transactions on Robotics*, vol. 33, no. 2, pp. 446–455, 2017.

[8] A. Jiang, T. Ranzani, G. Gerboni, L. Lekstutyte, K. Althoefer, P. Dasgupta, and T. Nanayakkara, "Robotic granular jamming: Does the membrane matter?," *Soft Robotics*, vol. 1, no. 3, pp. 192–201, 2014.

[9] E. Brown, N. Rodenberg, J. Amend, A. Mozeika, E. Steltz, M. R. Zakin, H. Lipson, and H. M. Jaeger, "Universal robotic gripper based on the jamming of granular material," *Proceedings of the National Academy of Sciences*, vol. 107, no. 44, pp. 18809–18814, 2010.

[10] K. Althoefer, "Antagonistic actuation and stiffness control in soft inflatable robots," *Nature Reviews Materials*, vol. 3, pp. 76–77, 04 2018.

[11] X. Jing, J. Jiang, F. Xie, C. Zhang, S. Chen, and L. Yang, "Continuum manipulator with rigid-flexible coupling structure," *IEEE Robotics and Automation Letters*, vol. 7, no. 4, pp. 11386–11393, 2022.

[12] D. Müller, A. Raisch, A. Hildebrandt, and O. Sawodny, "Nonlinear model based dynamic control of pneumatic driven quasi continuum manipulators," in *2020 IEEE/SICE International Symposium on System Integration (SII)*, pp. 277–282, 2020.

[13] C. Sun, L. Chen, J. Liu, J. S. Dai, and R. Kang, "A hybrid continuum robot based on pneumatic muscles with embedded elastic rods," *Proceedings of the Institution of Mechanical Engineers, Part C: Journal of Mechanical Engineering Science*, vol. 234, no. 1, pp. 318–328, 2020.

[14] C. Sozer, S. K. Sahu, L. Paternò, and A. Menciassi, "Robotic modules for a continuum manipulator with variable stiffness joints," *IEEE Robotics and Automation Letters*, vol. 8, no. 8, pp. 4745–4752, 2023.

[15] C. Christianson, N. N. Goldberg, D. D. Deheyn, S. Cai, and M. T. Tolley, "Translucent soft robots driven by frameless fluid electrode dielectric elastomer actuators," *Science Robotics*, vol. 3, no. 17, p. eaat1893, 2018.

[16] A. Stilli, H. A. Wurdemann, and K. Althoefer, "Shrinkable, stiffness-controllable soft manipulator based on a bio-inspired antagonistic actuation principle," in *2014 IEEE/RSJ International Conference on Intelligent Robots and Systems*, pp. 2476–2481, 2014.

[17] A. Shiva, A. Stilli, Y. Noh, A. Faragasso, I. D. Falco, G. Gerboni, M. Cianchetti, A. Menciassi, K. Althoefer, and H. A. Wurdemann, "Tendon-based stiffening for a pneumatically actuated soft manipulator," *IEEE Robotics and Automation Letters*, vol. 1, pp. 632–637, 2016.

[18] K. Suzumori, S. Wakimoto, K. Miyoshi, and K. Iwata, "Long bending rubber mechanism combined contracting and extending fluidic actuators," in *2013 IEEE/RSJ International Conference on Intelligent Robots and Systems*, pp. 4454–4459, 2013.

[19] M. E. Giannaccini, C. Xiang, A. Atyabi, T. Theodoridis, S. Nefti-Meziani, and S. Davis, "Novel design of a soft lightweight pneumatic continuum robot arm with decoupled variable stiffness and positioning," *Soft Robotics*, vol. 5, no. 1, pp. 54–70, 2018.

[20] L. A. Al Abeach, S. Nefti-Meziani, and S. Davis, "Design of a variable stiffness soft dexterous gripper," *Soft Robotics*, vol. 4, no. 3, pp. 274–284, 2017.

[21] Y. Zhang, W. Chen, J. Chen, Q. Cheng, H. Zhang, C. Xiang, and L. Hao, "Stiffness analysis of a pneumatic soft manipulator based on bending shape prediction," *IEEE Access*, vol. 8, pp. 82227–82241, 2020.

[22] H. Chen, Y. Ma, and W. Chen, "Design and optimization of an origami-inspired foldable pneumatic actuator," *IEEE Robotics and Automation Letters*, vol. 9, no. 2, pp. 1278–1285, 2024.

[23] J. Fang, J. Yuan, M. Wang, L. Xiao, J. Yang, Z. Lin, P. Xu, and L. Hou, "Novel accordion-inspired foldable pneumatic actuators for knee assistive devices," *Soft Robotics*, vol. 7, no. 1, pp. 95–108, 2020.

[24] B. Ugurlu, P. Forni, C. Doppmann, and J. Morimoto, "Torque and variable stiffness control for antagonistically driven pneumatic muscle actuators via a stable force feedback controller," in *2015 IEEE/RSJ International Conference on Intelligent Robots and Systems (IROS)*, pp. 1633–1639, 2015.

[25] J. Cao, S. Q. Xie, and R. Das, "Mimo sliding mode controller for gait exoskeleton driven by pneumatic muscles," *IEEE Transactions on Control Systems Technology*, vol. 26, no. 1, pp. 274–281, 2018.